Hindawi
International Journal of Optics
Volume 2022, Article ID 5734420, 14 pages
https://doi.org/10.1155/2022/5734420

Research Article

Performance Analysis of a Linear Gaussian- and tanh-Apodized FBG and Dispersion Compensating Fiber Design for Chromatic Dispersion Compensation in Long-haul Optical Communication Networks

Isidore Nsengiyumva,[1] **Elijah Mwangi**,[2] **and George Kamucha**[2]

[1]*Department of Electrical Engineering, Pan African University, Yaoundé, Cameroon*
[2]*Faculty of Engineering, University of Nairobi, Nairobi, Kenya*

Correspondence should be addressed to Isidore Nsengiyumva; isidore.nsengiyumva@students.jkuat.ac.ke

Received 4 March 2022; Revised 3 July 2022; Accepted 13 July 2022; Published 2 September 2022

Academic Editor: Yuan-Fong Chou Chau

This paper investigates a novel compensation technique of dispersion effect mitigation using a combination of three- and four-stage-apodized fiber Bragg gratings (FBG) and dispersion compensating fiber (DCF) designs. Two designs using three-stage and four-stage FBG and DCF in combination have been proposed and compared for their performance in mitigating chromatic dispersion effects at 100 km SMF. The performance of each design has been evaluated using Q-factor results using linear Gaussian- and tanh-apodized fiber Bragg gratings. Each profile manifested different Q-factor results over a range of 5 dBm, 7.5 dBm, and 10 dBm of CW laser power over FBG grating lengths from 4 mm to 8 mm. The results obtained using the three-stage and four-stage FBG and DCF designs showed that an apodization profile using a tanh function can be used successfully with FBG lengths from 4 mm to 8 mm, regardless of the CW launched power. In contrast, the results using a Gaussian apodization profile for three- and four-stage FBG and DCF designs are applicable to FBG lengths from 5 mm to 8 mm. Designs using three-stage FBG and DCF generated higher Q-factor results than designs using only four-stage FBG and DCF, regardless of the launched power. The highest Q-factor of 18.58 was obtained for three-stage tanh-apodized FBG and DCF used in combination for an FBG length of 6 mm. The highest result obtained for a three-stage Gaussian-apodized FBG and DCF design was a Q factor of 17.13 using an FBG length of 8 mm. The proposed method was also compared to current similar works and can be successfully implemented in long-haul optical communication.

1. Introduction

Fiber optic technology has become the de facto telecommunication system used to service the increasing demand for Internet traffic and high data rates. To achieve this objective, single and multimode fibers are applied, with conventional single-mode fiber (SMF) links being preferred for long-distance transmissions. However, signal strength attenuates with distance. The use of erbium-doped fiber amplifier (EDFA) has been reported to solve the problem of attenuation, especially in the C and L bands [1]. Various kinds of signal distortion happen when the signal strength is too high. The effects of nonlinearity can be effectively reduced by keeping the power level below certain limits or by using lasers with a flexible wavelength and broadband tuning range such as short-pulsed Raman fiber lasers [2]. Regardless of how narrow the laser linewidth is, any modulation scheme eventually widens due to intersymbol interference. Fiber dispersion effects have a range of 15–20 ps/nm/km and become more profound at long distances and higher transmission rates [3]. Laser sources are generally thin but not monochromatic. Chromatic dispersion is the most predominant form of dispersion in the fiber and occurs as the optical pulses inside the fiber

propagate at different speeds, thus leading to relative delays in arrival times [4].

There is extensive literature on practical and theoretical approaches to mitigation of chromatic dispersion effects [1, 5–8]. The dispersion compensating fiber (DCF) and the fiber Bragg grating (FBG) are most widely used in compensating the dispersion. The chirped FBG uses different apodization profiles to vary the period of the fiber grating in a linear, quadratic, or cubic manner. Linearly chirped Bragg gratings have been recognized in fiber optics as an effective dispersion-correcting and compensating approach [9]. Furthermore, chirped FBG has been reported to contribute to the generation of efficient and optimized high-power femtosecond pulses in mode-locked fiber lasers [10], and in the study and experimental observation of optical rogue waves (also known as "freak waves") [11].

The work in Reference [8] investigated the DCF technique to mitigate dispersion effects and obtained a Q-factor of 10.08 over a distance of 100 km using an FBG index of 2. However, overall cost and nonlinear effects were increased using DCF in the optical link. In Reference [7], an FBG index of 2 was used in simulations of an optical fiber link by shifting DCF and SMF relative positions to achieve precompensation, postcompensation, and symmetric compensation of dispersion effects. The postcompensation approach yielded Q-factor results of 41.40 for a single channel using a 10 Gb/s rate.

The work in Reference [12] investigated a double-stage hybrid DCF and a tanh function-apodized chirped FBG design to compensate for chromatic dispersion in a fiber link. An effective index of 1.45 was used in the experiment, and the Q factor and minimum BER results obtained were, respectively, 7.11 and 5.47033×10^{-13}.

Authors in Reference [13] investigated the time-domain equalization (TDE), frequency-domain equalization (FDE), the applied least mean square (LMS) adaptive equalization for the electronic dispersion compensation, and the DCF technique to mitigate optical dispersion. The research indicated that the choice of chromatic dispersion method severely affects the equalization enhanced phase noise (EEPN) as a result of the interaction between the electronic dispersion compensation and the laser source noise.

The paper in Reference [14] proposed a design and simulation framework using a combination of EDFA and FBG for uniform, Gaussian, and tanh apodization profiles over a 50 km, 60 km, 70 km, and 80 km eight-channel wavelength division multiplexed (WDM) link. A range of FBG lengths from 5 mm to 10 mm were investigated, and the highest Q-factor result obtained was 29.70 dBm at 10 mm.

In Reference [15], different chirps using linear, cubic, or uniform profiles were applied to FBG in conjunction with DCF to improve the efficiency in pulse width reduction (PWR). However, a dispersion compensating module design using a linear combination of double stage FBG and DCF revealed a performance of 98% in terms of PWR efficiency. In contrast, other modules using simply DCF or a combination of single FBG and DCF were less efficient.

This work investigates the performance of multistage FBG and DCF in combination using three and four elements of FBG, respectively. An FBG grating index of 1.46 is less prevalent in literature and was used throughout the investigation. The aim is to improve the link's transmission quality by mitigating the effects of chromatic dispersion further.

The rest of this paper is organized as follows: Section 2 presents the mathematical analysis of DCF and chirped fiber Bragg grating. Section 3 covers the experimental setup of proposed designs and the important parameters used in simulation. A discussion of the results and comparison with similar works is covered in Section 4, while Section 5 presents the conclusion of the research investigation.

2. Mathematical Analysis

2.1. Theory and Principle of the Dispersion Compensating Fiber. The use of DCF significantly improves the behavior of SMF transmissions. A fiber with a reversed dispersion coefficient is known as a dispersion compensating fiber. The conventional DCF has dispersion values in the range of −70 to −90 psi/(nm km). Despite being expensive, the DCF is ideally one of the most efficient methods for chromatic dispersion compensation in which an SMF is concatenated with a DCF whose dispersion-length product is the additive inverse of that of the SMF, hence reducing the overall equivalent dispersion of the optical communication link ideally to zero [12]. However, DCF also has limitations in the form of nonlinearities, high-order dispersion, and cannot be tuned. Fiber Bragg gratings offer an alternative approach to the challenges of using DCF. Furthermore, using the chirped FBG as a dispersion compensation module reduces the cost substantially as compared to the cost of DCF [16].

The condition for obtaining zero dispersion slopes at the operating wavelength of a link composed of SMF and DCF is that the relative dispersion slope (RDS) of the DCF should be equal to the RDS of the SMF at the operating wavelength [17]. The relationship between the positive dispersion of SMF and the negative dispersion of DCF is given by equation (1) as in Reference [8] or Reference [16] by equation (1).

$$D_{\mathrm{SMF}} L_{\mathrm{SMF}} + D_{\mathrm{DCF}} L_{\mathrm{DCF}} = 0, \tag{1}$$

where L_{SMF} and L_{DCF} represent the lengths of SMF and DCF, respectively.

The dispersion of a concatenated SMF–DCF fiber link can be characterized by an equivalent dispersion $D_{\mathrm{eq}}(\lambda)$ as in Reference [18] given by equation (2):

$$D_{\mathrm{eq}}(\lambda) = \frac{\left[R D_{\mathrm{SMF}} + D_{\mathrm{DCF}}(\lambda)\right]}{(1+R)}, \tag{2}$$

where R is the length ratio of the SMF to the DCF, and D_{SMF} and D_{DCF} are the respective dispersions of the SMF and DSF segments.

From equation (2), given D_{eq} as zero fulfills the ideal dispersion compensation condition expressed by equation (1). A dispersion compensation rate at a wide wavelength range is given by equation (3) as in Reference [17]:

$$\text{compensation rate}(\%) = \frac{(\text{Slope}_{\text{DCF}}/\text{Slope}_{\text{SMF}})}{(\text{Dispersion}_{\text{DCF}}/\text{Dispersion}_{\text{SMF}})}, \tag{3}$$

where slope is defined as the difference of dispersion values per a wavelength interval.

2.2. Theory and Principle of Chirped Fiber Bragg Grating. Using a combination of FBG and DCF, it is possible to take advantage of both the features of DCF and FBG. Fiber gratings are tunable and can have uniform or nonuniform periods. Furthermore, fiber gratings generally take many forms where the period may vary linearly, randomly, or have a quadratic or cubic shape.

A fiber Bragg grating (FBG) is a small uniform segment of optical fiber having a periodic disparity in refractive index besides an axis of fiber length, which is created through exposing the photosensitive optical fiber to an ultraviolet light ray [19]. Chirped gratings have a nonuniform period along their length as illustrated in Figure 1.

Fiber Bragg gratings behave like a band-stopping filter in the sense that they reflect any wavelength that satisfy Bragg's condition (equation (4)) and propagate remaining wavelengths [20]. A coupler is used to separate incident wavelengths from reflected pulses.

$$\lambda_{\text{Bragg}} = 2 \cdot n_{\text{eff}} \cdot \Lambda, \tag{4}$$

where λ_{Bragg} is Bragg's reflecting wavelength, n_{eff} the effective refractive index of the fiber core, and Λ is the grating period of the fiber.

The range of all reflected wavelengths $\Delta\lambda_{\text{chirp}}$ due to the introduction of chirped FBG is expressed by equation (5) as shown in Reference [21].

$$\Delta\lambda_{\text{chirp}} = 2n_{\text{eff}} \cdot \left(\Lambda_{\text{long}} - \Lambda_{\text{short}}\right), \tag{5}$$

where Λ_{long} and Λ_{short} are the longest and shortest wavelength, respectively.

The time delay $\tau(\lambda)$ for each wavelength along the chirped FBG can be computed using equation (6) as shown in [22].

$$\tau(\lambda) = \left(\lambda_{\text{Bragg}} - \lambda\right)\frac{2n_{\text{eff}}}{\Delta\lambda c} \cdot L_g, \tag{6}$$

where L_g is the length of the fiber grating and c is the speed of light.

The time delay can also be expressed generally by equation (7) as shown in Reference [16].

$$\tau(\lambda) = \frac{\left(\lambda_{\text{Broad}} - \lambda_{\text{Bragg}}\right)}{\left(\Lambda_{\text{long}} - \Lambda_{\text{short}}\right)} \cdot \frac{2n_{\text{eff}}L_g}{c}, \tag{7}$$

where $(\Lambda_{short} \le \lambda \le \Lambda_{long})$.

The dispersion of the chirped FBG is calculated using equation (8) as shown in Reference [19].

$$D(\lambda) = \frac{d\tau(\lambda)}{d(\lambda)} = \frac{1}{\left(\Lambda_{\text{long}} - \Lambda_{\text{short}}\right)} \cdot \frac{2n_{\text{eff}}L_g}{c}. \tag{8}$$

For a laser source spectrum with a width $\Delta\Lambda$, propagated through a fiber of length L, the overall chromatic dispersion is also related to the total delay $\Delta\tau$ in the fiber as shown in Reference [23].

$$\frac{\Delta\tau}{L} = D_{ch}(\Delta\Lambda), \tag{9}$$

where D_{ch} is the total chromatic dispersion inside the fiber.

The performance of the system is generally expressed in terms of BER, but the Q-factor measurement based on the assumption of normal noise distribution adopts the concept of S/N ratio to evaluate the system performance [24]. The BER of the system can be determined using the Q factor using equation (10) as shown in Reference [24].

$$\text{BER} = \frac{1}{2}\text{erfc}\left(\frac{Q}{\sqrt{2}}\right). \tag{10}$$

For a resonant frequency f_0 where $Q = 2\pi f_0$, BER can computed from the Gaussian approximation by equation (11)

$$\text{BER} \approx \frac{\exp\left(-\left(Q^2/2\right)\right)}{Q\sqrt{2\pi}}. \tag{11}$$

Several apodization functions have been proposed to improve the performance of fiber transmissions using Bragg's gratings for chromatic dispersion compensation [25]. Apodization reduces internal interference effects due to group delay, and chirped gratings offer ideal properties for the linear compensation of dispersion in fibers [9]. The Gaussian-apodized and *tanh*-apodized FBG have been reported to have optimum performance in terms of side lobe suppression and maximum reflectivity [26].

When a frame of reference along the z-line is considered, a linear variation from a period Λ_0 to Λ_z is represented by equation (12):

$$\Lambda(z) = \Lambda_0 + xz. \tag{12}$$

The relationship between the apodization function $g(z)$ and the refractive index $n(z)$ of the fiber is defined as shown in Reference [27].

$$n(z) = n_{\text{eff}} + \Delta n g(z)\cos\left(\frac{2\pi z}{\Lambda_0}(1 + xz)\right), \tag{13}$$

where Δn is the average change in the index modulation.

The performance of the proposed designs will be evaluated using Gaussian and tanh apodization profiles as in Reference [14] using equations (14) and (15) for Gaussian and tanh functions, respectively.

$$T(z) = \exp\left[-G\left(\frac{z}{L_g}\right)^2\right], \tag{14}$$

$$T(z) = 1 + \tanh\left[T\left(1 - 2\left(\frac{z}{L_g}\right)^2\right)\right], \tag{15}$$

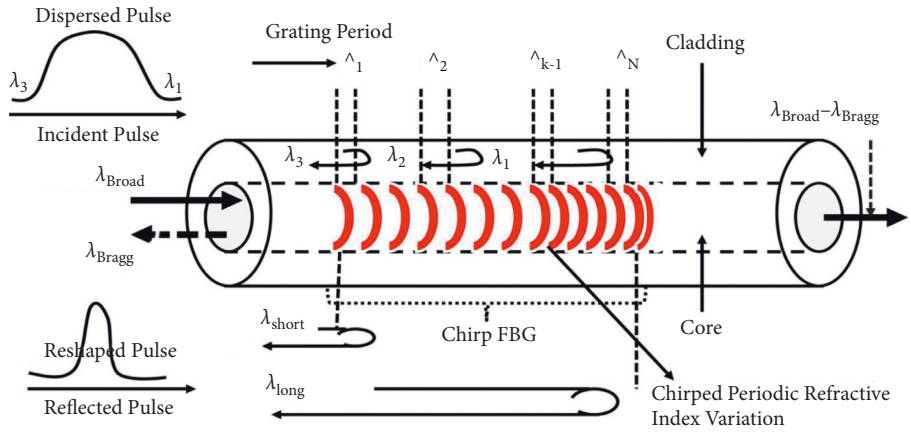

Figure 1: Nonuniform fiber Bragg gratings [19].

where parameters G and T are used to control the apodization sharpness parameter and L_g the grating length.

The grating length L_g is calculated using the geometric expression in equation (16):

$$L_g = \Lambda_1\left(\frac{1-M^N}{1-M}\right), \tag{16}$$

where Λ_1, M, and N are the initial phase, linear change in phase, and the number of grating period, respectively.

3. Proposed Design and Simulation Framework

The Optisystem 18 [28] software is used to evaluate the performance of the two design models using a hybrid DCF and chirped linear three-stage and four-stage FBG in combination. Simulations are used because practical implementation of the proposed designs carries a huge financial cost.

This work investigates design models incorporating three and four stages of linear chirped FBG in combination with DCF, respectively, at 100 km of SMF. Assuming a dispersion slope of 16 psi/(nm km), the total dispersion at 100 km becomes 1600 psi/(nm km), and a DCF length of 20 km is required to yield optimum performance according to equation (1). However, the system in Reference [15] obtained a pulse width reduction efficiency of approximately 98% using only 11.5 km of DCF length. The proposed designs employ a cascade of three and four FBG to determine the improvement in Q-factor and BER.

Each link is generally composed of a transmitter with a frequency of 193.1 THz, a receiver, and the dispersion module under investigation. The dispersion module consists of three or four stages of linear chirped FBG. The transmitter is composed of a laser and data source, a nonreturn to zero (NRZ) pulse generator, and a Mach–Zehnder modulator. The modulator has an extinction ratio of 30 dB and generates a pulse width of 100 ps. The launched power is varied from 5 dBm to 10 dBm power range to capture the variations of Q factor and simultaneously limit nonlinear effects due to launch power increase. The optical receiver incorporates a PIN detector, a 3R regenerator, and a Bessel filter. The 3R regenerator element is used to simplify the proposed simulation model and performs three main operations: regeneration of the amplitude, the signal waveform, and synchronization of the received signal. The simulation design model using three-stage FBG and DCF is shown in Figure 2 whereas Figure 3 corresponds to the proposed simulation model for four-stage FBG and DCF used in combination.

After amplification, the received optical pulse is detected by the positive intrinsic negative (PIN) photo detector and smoothed through a low-pass filter. The measured results are shown on the BER analyzer in the form of a Q factor and a BER diagram.

Parameters used to investigate the performance of the proposed models are given in Table 1.

4. Results and Discussion

A model using a single apodized FBG and DCF was used in Reference [12] for a length of 300 km. The authors in Reference [15] used a model consisting of a hybrid DCF and two consecutive FBG modules to mitigate dispersion effects on a 100 SMF km link. The investigation in Reference [15] used an FBG length of 70 mm, and the results were obtained using a CW power of 0 dBm. Using the design proposed in Reference [15], the Q-factor results obtained using launched power ranging from 0 dBm to 10 dBm at an FBG length of 4 mm are recorded in Table 2. The Q-factor results obtained using launched power between 5 dBm and 10 dBm satisfy the minimum theoretical standard requirement of $Q > 6$.

In the remainder of this investigation, a CW laser power of 5 dBm, 7.5 dBm, and 10 dBm has been chosen to conduct the performance analysis of the link using an FBG grating length varying from 4 mm to 8 mm. The FBG grating length range was chosen to maximize the output Q factor and in

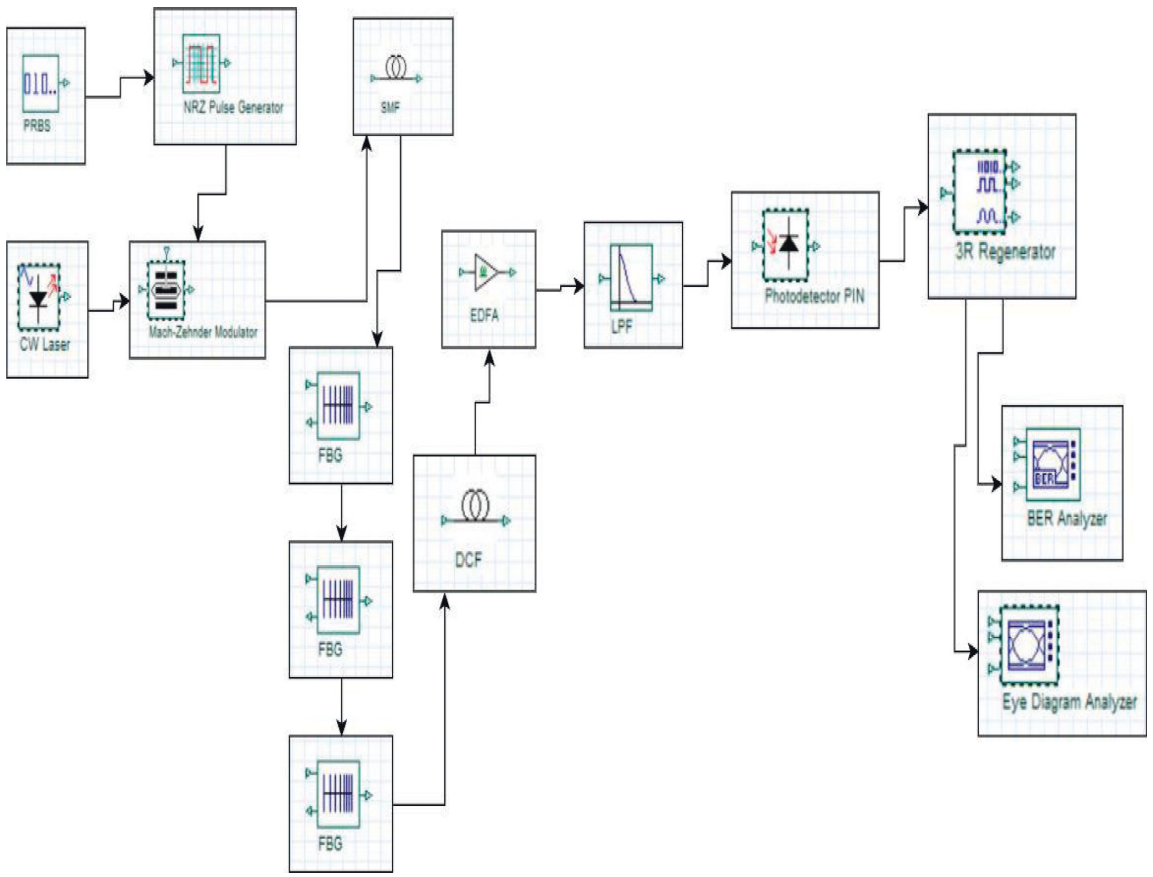

Figure 2: A cascade of three stage FBG and DCF simulation model at 100 km of SMF.

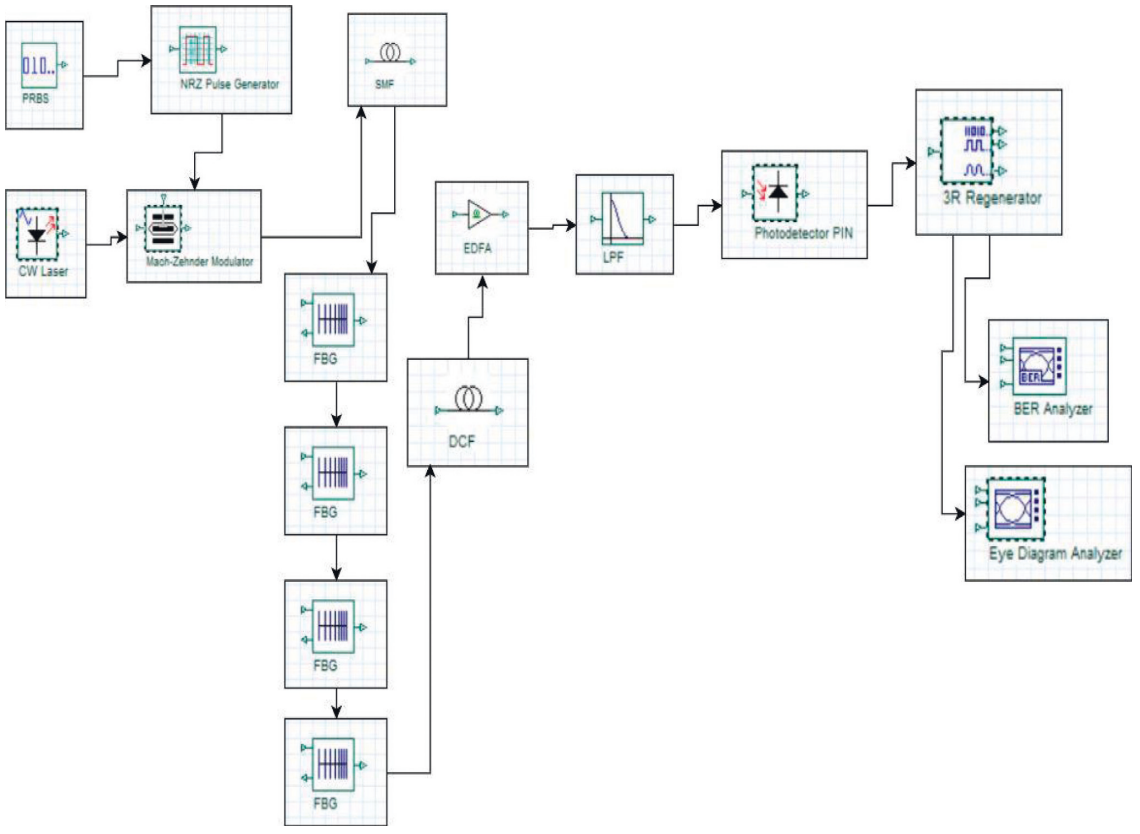

Figure 3: A cascade of four stage FBG and DCF simulation model at 100 km of SMF.

Table 1: Parameters used in simulation.

Transmission medium	Parameters
CW laser power	Linewidth: 10 MHz Frequency: 193.1 THz Launched power: 5 dBm, 7.5 dBm, 10 dBm
Optical fibre	Attenuation: 0.2 dB/km Length: 100 km Dispersion: 16 ps/nm/km
DCF fibre	Length: 11.5 km Dispersion slope: −0.3 ps/nm^2/km Dispersion: −80 ps/nm/km
Chirped FBG	Index: 1.46

Table 2: Q factor versus CW laser power for [15].

Power in dBm	Q factor
5	5.95
7.5	6.82
10	8.94

Table 3: Q-factor results for 3 FBG + DCF linear Gaussian apodization simulation models.

FBG length in mm	Q factor at 5 dBm	Q factor at 7.5 dBm	Q factor at 10 dBm
4	5.13	6.52	8.37
5	6.91	7.00	10.81
6	9.22	9.50	13.06
7	10.71	13.42	15.17
8	12.32	14.01	17.13

Table 4: Q-factor results for 3 FBG + DCF linear tanh apodization simulation models.

FBG length in mm	Q factor at 5 dBm	Q factor at 7.5 dBm	Q factor at 10 dBm
4	10.22	11.05	13.06
5	11.63	11.99	14.94
6	13.16	14.24	18.58
7	13.04	15.61	17.29
8	13.40	15.80	17.81

conforming to the Q-factor standard requirement to achieve optimum transmissions.

Two linear chirp profiles have been used to evaluate the performance of a hybrid multistage FBG and DCF design in mitigating dispersion effects using 100 km of SMF length, and a DCF length of 11.5 km to preserve the pulse width reduction ratio obtained in Reference [15]. Different Q-factor results were obtained when using a cascade of three FBG and DCF using a linear chirped Gaussian and tanh function, respectively. Table 3 illustrates the results of a linear Gaussian chirp for a design using three cascaded FBG and DCF.

Results of the tanh linear chirp profile using a cascade of three FBG and DCF are shown in Table 4.

Depending on the CW power and the chirp profile used, the Q factor manifests differently. The results obtained using linear chirped Gaussian and tanh profiles differ for 5 dBm, 7.5 dBm, and 10 dBm power in the first design using three FBG and DCF. The Q-factor results were obtained for different FBG lengths varying from 4 mm to 8 mm. Higher Q-factor results are generally obtained using high launched power and are slightly higher for a tanh apodization profile than for a Gaussian apodization profile as illustrated in Figure 4.

A comparison of the performance of the three FBG cascade and DCF designs for linear chirp Gaussian and tanh profiles are given in Figure 5, respectively, for 5 dBm, 7.5 dBm, and 10 dBm CW laser power. At 5 dBm, Q-factor

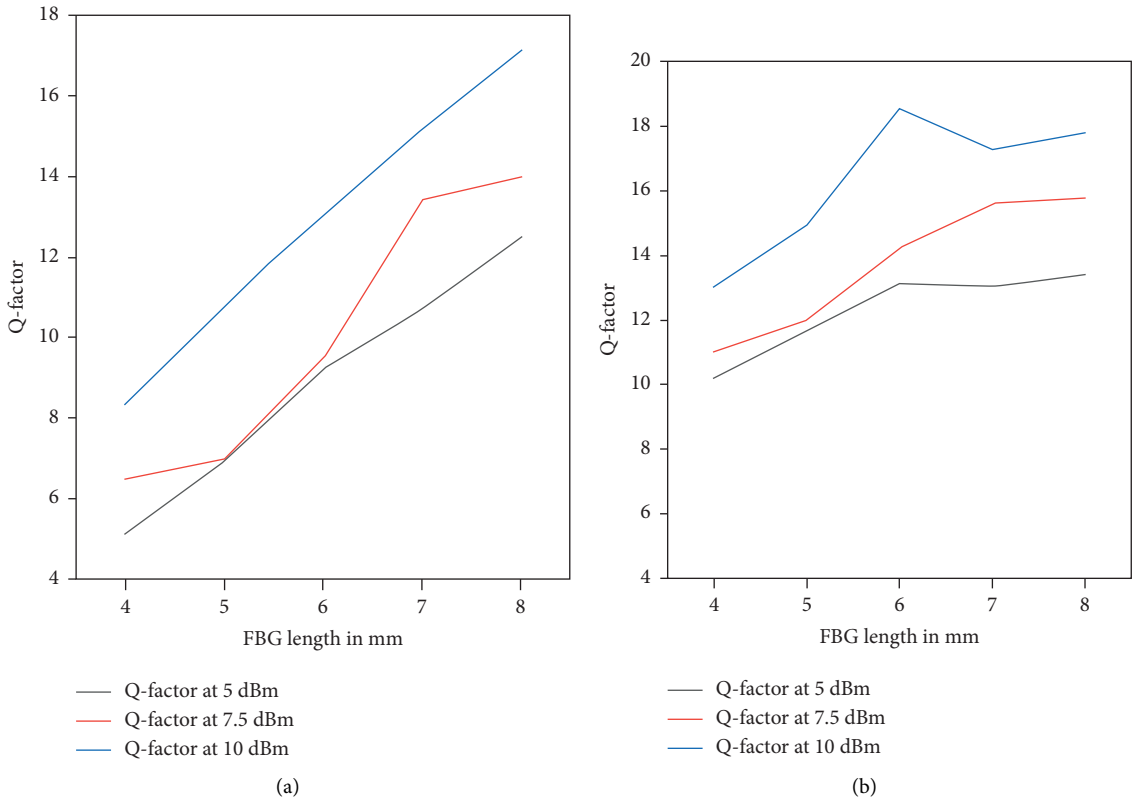

Figure 4: A comparison of Q-factor results for 5 dBm, 7.5 dBm, and 10 dBm for 3 FBG + DCF: (a) Gaussian profile and (b) tanh profile.

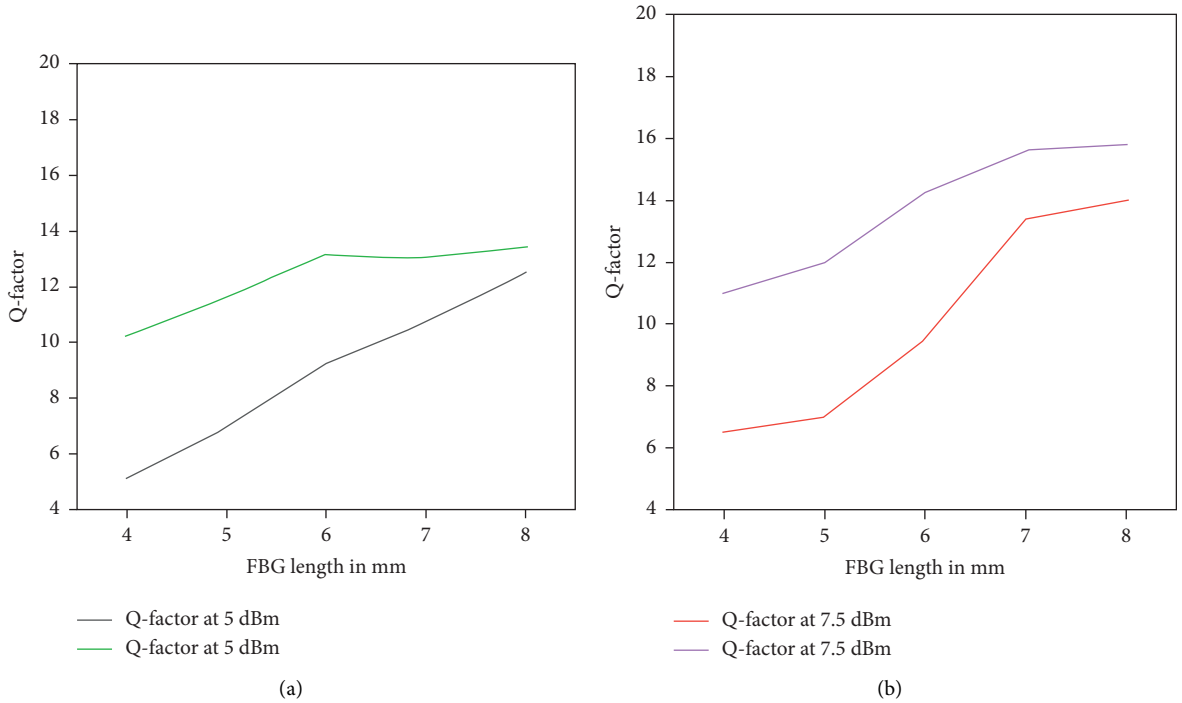

Figure 5: Continued.

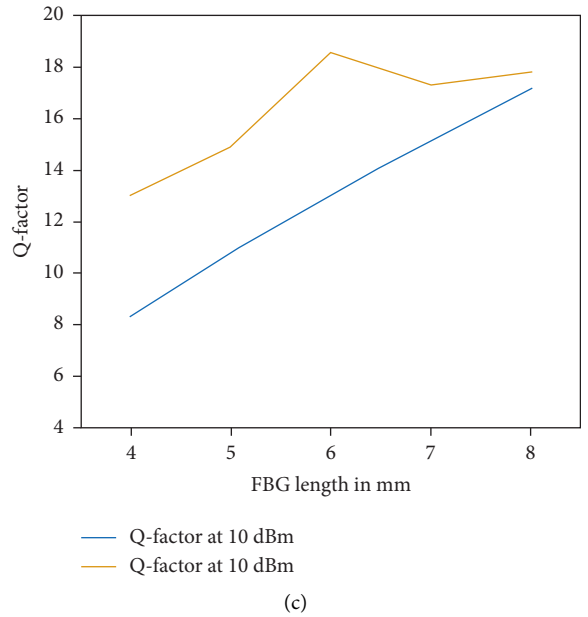

(c)

Figure 5: Comparison of linear Gaussian versus linear tanh profile 3 FBG + DCF. (a) for 5 dBm, (b) for 7.5 dBm, and (c) for 10 dBm.

Table 5: Q-factor results for 4 FBG + DCF linear tanh apodization simulation models.

FBG length in mm	Q factor in 5 dBm	Q factor at 7.5 dBm	Q factor at 10 dBm
4	8.13	9.52	10.95
5	9.06	10.81	11.34
6	8.56	8.69	12.52
7	6.76	7.96	9.08
8	5.23	6.83	6.69

Table 6: Q-factor results for 4 FBG + DCF linear Gaussian apodization simulation models.

FBG length in mm	Q factor in 5 dBm	Q factor at 7.5 dBm	Q factor at 10 dBm
4	4.23	6.15	7.99
5	6.21	7.03	9.75
6	7.73	8.19	11.68
7	8.58	9.74	12.44
8	9.23	10.78	12.80

results are higher when using linear tanh chirp than when using a linear chirped Gaussian FBG regardless of its length as shown in Figure 5(a). The same is true for a CW launched power of 7.5 dBm and 10 dBm as shown by Figure 5(b) and Figure 5(c), respectively.

The second design uses a cascade of four-stage FBG and DCF for linear Gaussian and tanh apodization profiles. Results for the tanh apodization profile obtained for this design are recorded in Table 5.

The Q-factor results obtained using launched power of 5 dBm, 7.5 dBm, and 10 dBm for the Gaussian profile are recorded in Table 6, respectively.

These results agree with theoretical predictions and show that a design of three- or four-stage Gaussian chirped FBG and DCF can be used successfully for FBG grating lengths between 5 mm and 8 mm to carry transmissions at 100 km. A cascaded FBG design can be used successfully to reduce the used spectral width of the transmitted optical signal and consequently reduce the propagation delay and improve system performance [27]. Furthermore, the tanh profile yields slightly higher results than the Gaussian profile over the same distance in the window that uses grating lengths between 4 mm and 8 mm. Outside of that window, the Q factor obtained is below the theoretical standard

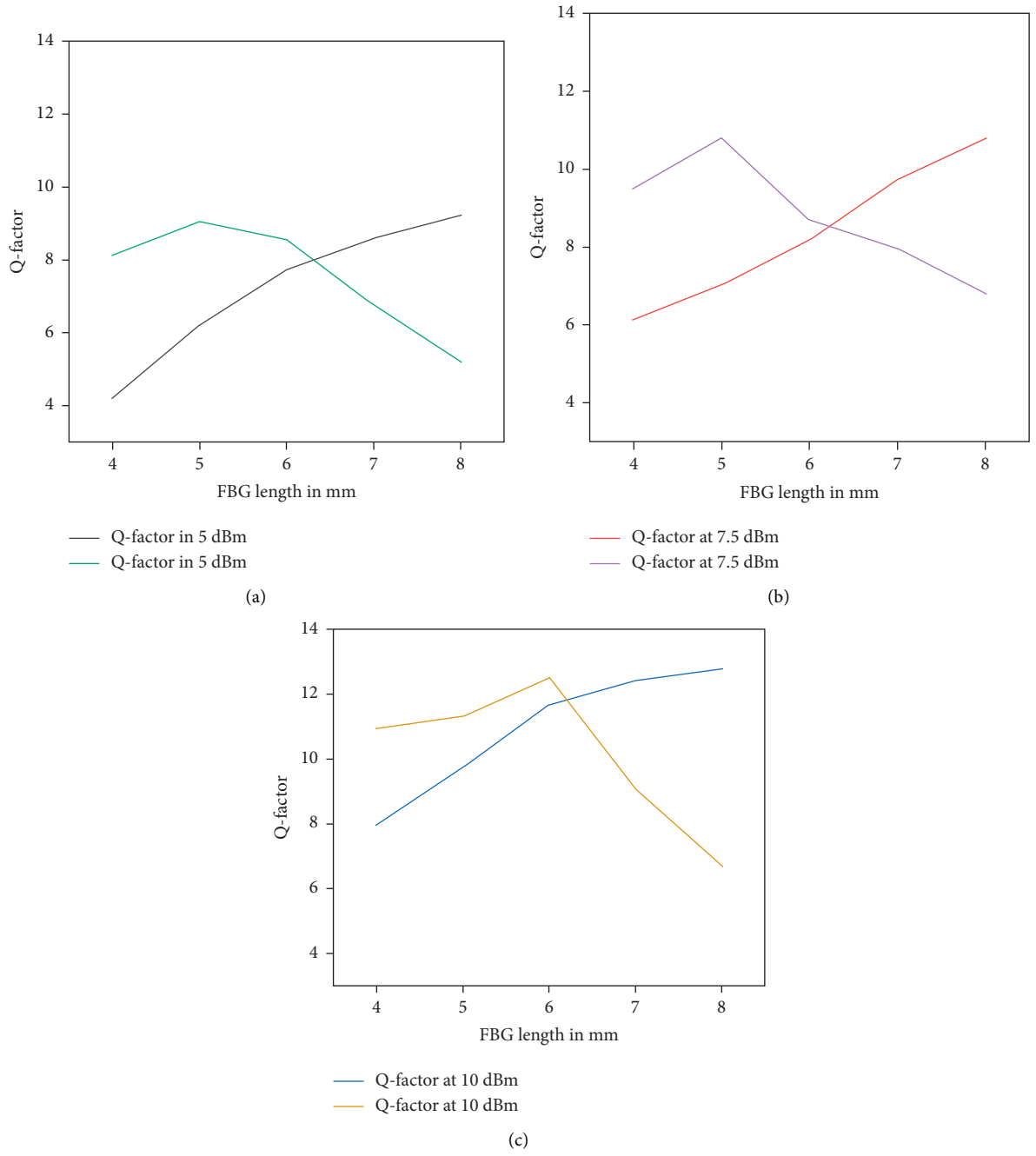

Figure 6: Comparison of linear Gaussian versus linear tanh profile 4 FBG + DCF. (a) for 5 dBm, (b) for 7.5 dBm, (c) for 10 dBm.

requirement of $Q \geq 6$. The dispersion compensation process using chirped FBG enhances receiver performance, and the reflectivity improves as the number of stages increases [27]. However, Gaussian apodization requires a low power level, shows better performance in terms of the side lobes and full-width–half-maximum (FWHM), and has better reflectivity than tanh apodization [29]. A comparison of Q-factor results for the four-stage FBG and DCF designs using Gaussian- and tanh-apodized fibers for varying injected power values of 5 dBm, 7 5 dBm, and 10 dBm is illustrated in Figure 6, respectively. As the injected power increases, the Q factor consistently increases for the

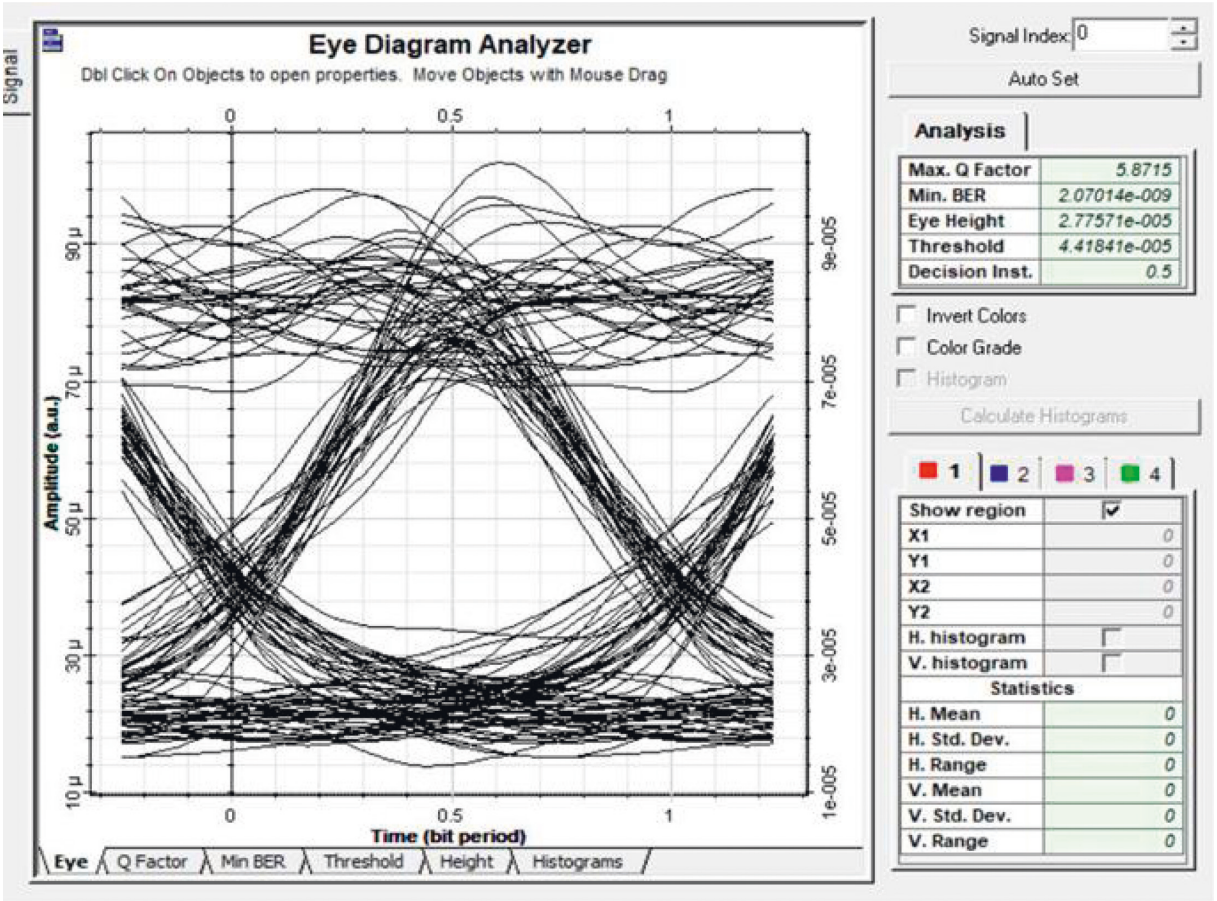

Figure 7: Eye-diagram graphs for single-stage Gaussian-apodized FBG + DCF design.

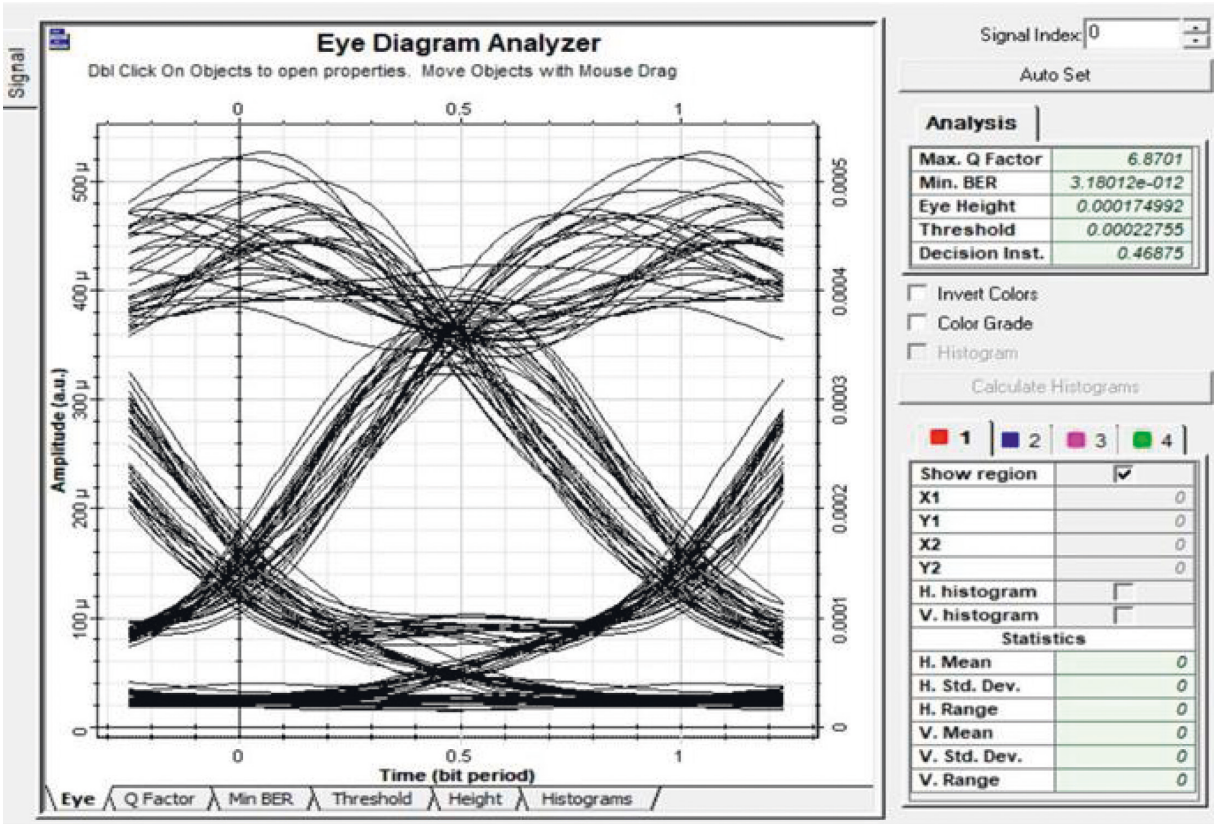

Figure 8: Eye-diagram graphs for double-stage Gaussian-apodized FBG + DCF design.

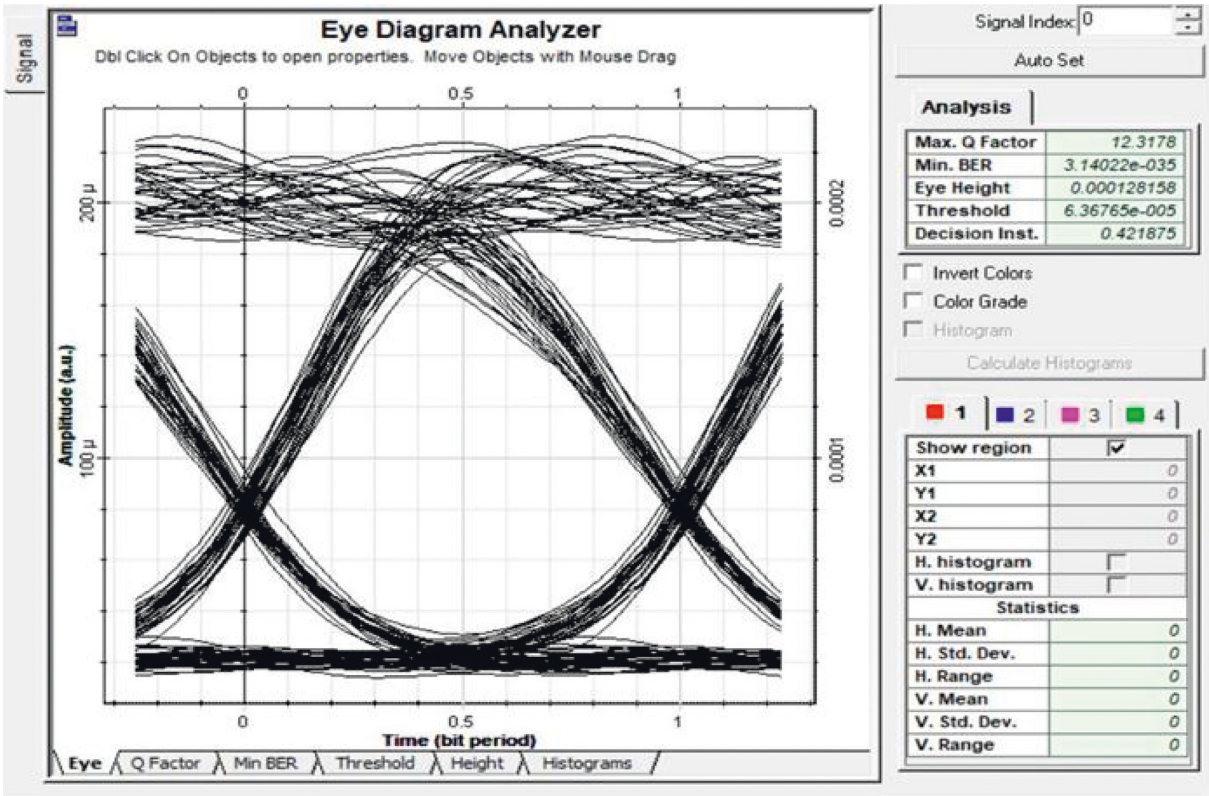

Figure 9: Eye-diagram graphs for three-stage Gaussian-apodized FBG + DCF design.

Gaussian apodization and slightly decreases for the tanh profile due to strain and self-phase modulation. From a launch power of 7.5 dBm to 10 dBm, the Q factor consistently increases.

(See Figures 7–10) give a comparison of obtained eye-diagram graphs for single-, double-, three-, and four-stage designs using apodized FBG, respectively. Eye diagrams are obtained for a grating length of 8 mm using a fiber index of $n = 1.46$ and a launch power of 5dBm. Q-factor results obtained for single stage is small compared to the Q-factor result obtained in Figure 9 for three-stage designs. Similarly, the Q-factor result obtained in Figure 8 for a double stage design is greater than that obtained in Figure 7 using a single stage design owing to the increased filtering capacity. Multistage designs using FBG increase the cost due to the need for more FBG modules. However, our proposed designs require shorter apodized FBG than the designs available in References [15, 30] and produce Q-factor results that match the required Q-factor value for optimal optical communications.

Obtained results can also be compared with other available similar research using one or multiple stage designs of FBG and DCF in combination. For a launch power of 5 dBm, the results obtained for the three-stage design of FBG and DCF used in combination is compared with results obtained in References [3, 15, 19, 30] on the basis of Q-factor results, BER, and eye-diagrams. A comparison of the proposed design using Q-factor results and corresponding BER is provided in Table 7.

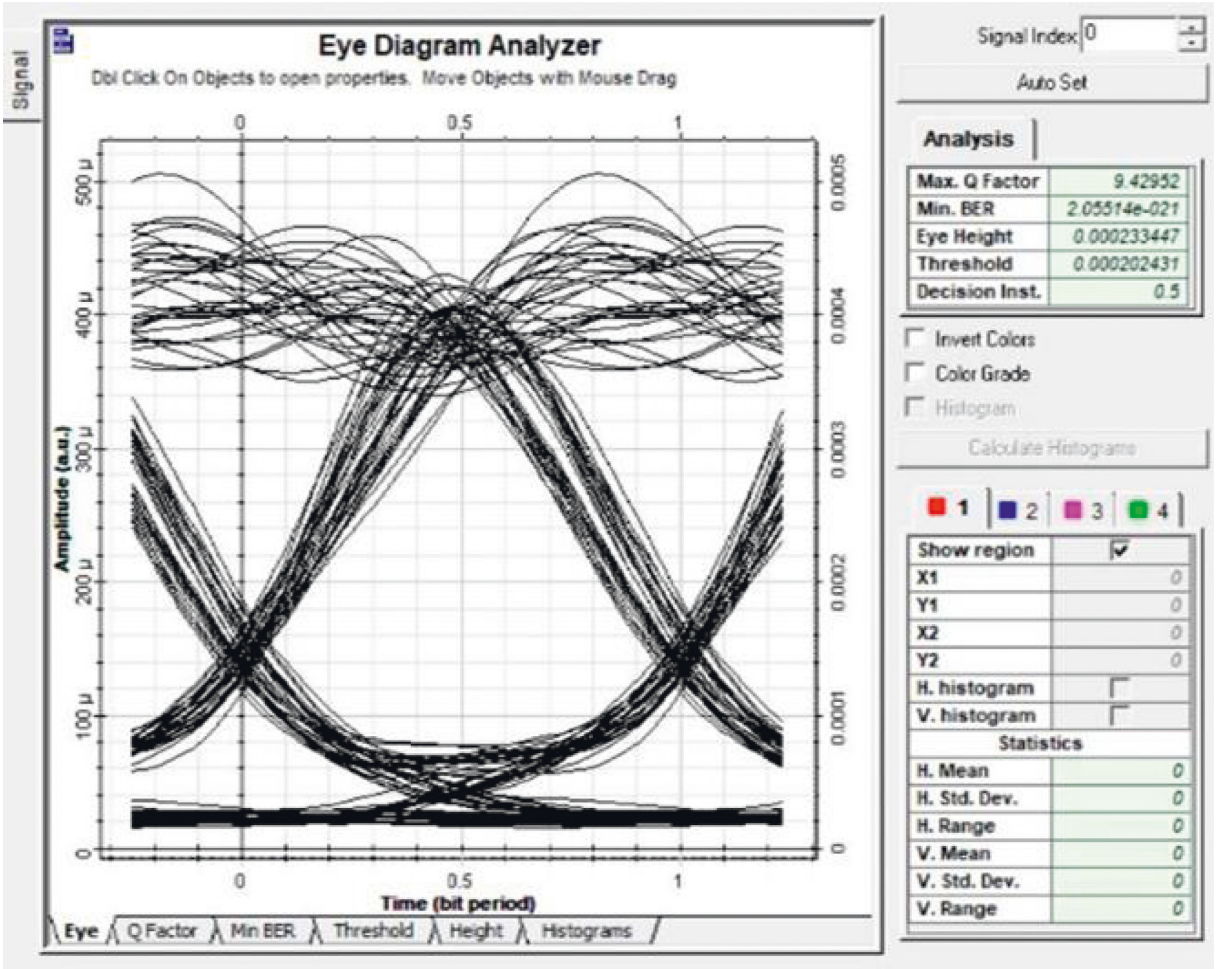

Figure 10: Eye-diagram graph for four-stage Gaussian-apodized FBG + DCF design.

Table 7: Comparison of different designs using the apodized chirped Gaussian profile.

References	FBG refractive index	SMF in km	Gaussian-apodized CFBG length in mm	Quality factor in dBm	BER
[3]	1.45	210	87	23.14	7.04×10^{-11}
[19]	1.47	150	45	12.74	1.63×10^{-37}
[15]	2	100	70	5.95	9.51×10^{-21}
[30]	1.46	150	8	3.39	4.51×10^{-35}
This work	1.46	100	8	12.48	3.15×10^{-45}

5. Conclusion

This paper proposed a combination of multistage apodized FBG and DCF design for the mitigation of chromatic dispersion at 100-km SMF link. Two apodization profiles using Gaussian and tanh functions were used and compared over FBG lengths from 4 mm to 8 mm using CW power of 5 dBm, 7.5 dBm, and 10 dBm, respectively. The minimum FBG length was generally found to be at least 4 mm regardless of the apodization profile used. However, Q-factor results obtained showed that the tanh apodization profile is suitable for FBG lengths from 4 mm to 8 mm, while the Gaussian apodization profile can be successfully used in designs using FBG lengths from 5 mm to 8 mm. The proposed designs can be successfully used to carry loads of data over long distances. The Q-factor results obtained using the multistage FBG and DCF incorporating three and four elements of FBG are twice those obtained for a design using only two elements of FBG and DCF in combination. This presents an opportunity for mitigating chromatic dispersion effects and must be investigated further to determine the effects of reflection on the overall performance of the designs as dispersion compensation modules are increased. Increasing the stages of chirped FBG coupled with an increase in the injected power generally increases the overall quality factor. However, as the stages increase, the use of chirped FBG and DCF in combination suffers from nonlinear effects. This could be the subject of future research.

Data Availability

The data used to support the findings of this study are included within the article.

Conflicts of Interest

The authors declare that they have no conflicts of interest.

Acknowledgments

The authors acknowledge the African Union Commission for funding this work through the Pan African University Scholarship Programme. The authors also thank the Burundi Ministry of National Defence and Veterans' Affairs for the support received during the final stage of the research.

References

[1] A. Sharma, I. Singh, S. Bhattacharya, and S. Sharma, "Performance comparison of DCF and FBG as dispersion compensation techniques at 100 Gbps over 120 km using SMF," *Nanoelectronics, Circuits and Communication Systems*, pp. 435–449, Springer Nature Singapore Pte Ltd, Singapore, 2019.

[2] J. Liu, J. Wu, H. Chen et al., "Short-pulsed Raman fiber laser and its dynamics," *Science China Physics, Mechanics & Astronomy*, vol. 64, no. 1, pp. 1–21, Article ID 214201, 2021.

[3] R. Gupta and M. L. Meena, "Long-distance optical communication network with linear chirped fiber Bragg grating," *Machine Intelligence and Smart Systems (MISS): Proceedings of MISS 2020*, pp. 185–192, Springer, Gateway East, Singapore, 2020.

[4] J. Wang, X. Jiang, X. He, and Z. Pan, "Ultra-wide range in-service chromatic dispersion measurement using coherent detection and digital signal processing," in *Proceedings of the SPIE (Optica Publishing Group, 2011)*, Shangai, China, 2011.

[5] S. Ranathive, K. Vinoth Kumar, A. N. Z. Rashed, M. S. F. Tabbour, and T. Sundararajan, "Performance signature of optical fiber communications dispersion compensation techniques for the control of dispersion management," *Journal of Optical Communications*, vol. 0, no. 0, pp. 1–13, 2019.

[6] A. B. Dar and R. K. Jha, "Chromatic dispersion compensation techniques and characterization of fiber Bragg grating for dispersion compensation," *Optical and Quantum Electronics*, vol. 49, no. 3, pp. 108–135, 2017.

[7] M. B. Hossain, A. Adhikary, and T. Z. Khan, "Performance investigation of different dispersion compensation methods in optical fiber communication," *Asian Journal of Research in Computer Science*, vol. 5, no. 2, pp. 36–44, 2020.

[8] A. H. Ali, S. H. Abdulwahed, and M. A. Al-Ja`afari, "Investigation of the different compensation methods for single optical channel," *Journal of Engineering and Applied Sciences*, vol. 14, no. 9, pp. 3018–3022, 2019.

[9] R. Kashyap, "Chirped fiber Bragg gratings," *Fiber Bragg Gratings*, pp. 305–307, Elsevier, Amsterdam, Netherlands, 2010.

[10] Y. Han, Y. Guo, B. Gao, C. Ma, R. Zhang, and H. Zhang, "Generation, optimization, and application of ultrashort femtosecond pulse in mode-locked fiber lasers," *Progress in Quantum Electronics*, vol. 71, pp. 1–35, 2020.

[11] Y. Song, Z. Wang, C. Wang, K. Panajotov, and H. Zhang, "Recent progress on optical rogue waves in fiber lasers: status, challenges, and perspectives," *Advanced Photonics*, vol. 2, no. 02, Article ID 024001, 2020.

[12] T. F. Hussein, M. R. M. Rizk, and M. H. Aly, "A hybrid DCF/FBG scheme for dispersion compensation over a 300 km SMF," *Optical and Quantum Electronics*, vol. 51, no. 4, pp. 103–116, 2019.

[13] T. Xua, G. Jacobsenb, S. Popovb et al., "Analysis of chromatic dispersion compensation and carrier phase recovery in long-haul optical transmission system influenced by equalization enhanced phase noise," *Optik*, vol. 138, pp. 494–508, 2017.

[14] D. Ahlawat, P. Arora, and S. Kumar, "Performance evaluation of proposed WDM optical link using EDFA and FBG combination," *Journal of Optical Communications*, vol. 40, no. 2, pp. 101–107, 2019.

[15] S. Aggarwal, N. Garg, and G. Kaur, "Performance Evaluation of Various Dispersion Compensation Modules," *Wireless Personal Communications*, vol. 123, pp. 1–15, 2021.

[16] N. A. Mohammed, M. Solaiman, and M. H. Aly, "Design and performance evaluation of a dispersion compensation unit using several chirping functions in a tanh apodized FBG and comparison with dispersion compensation fiber," *Applied Optics*, vol. 53, no. 29, pp. H239–H247, 2014.

[17] K. Xu and Y. Ou, "Theoretical and numerical characterization of a 40 Gbps long-haul multi-channel transmission system with dispersion compensation," *Digital Communications and Networks*, vol. 1, no. 3, pp. 222–228, 2015.

[18] C.-C. Chang, A. M. Vengsarkar, D. W. Peckham, and A. M. Weiner, "Broadband fiber dispersion compensation for sub-100-fs pulses with a compression ratio of 300," *Optics Letters*, vol. 21, no. 15, pp. 1141-1142, 1996.

[19] M. Meena and R. Kumar Gupta, "Design and comparative performance evaluation of chirped FBG dispersion compensation with DCF technique for DWDM optical transmission systems," *Optik*, vol. 188, pp. 212–224, 2019.

[20] N. A. Mohammed, T. A. Ali, and M. H. Aly, "Evaluation and performance enhancement for accurate FBG temperature sensor measurement with different apodization profiles in single and quasi-distributed DWDM systems," *Optics and Lasers in Engineering*, vol. 55, pp. 22–34, 2014.

[21] H. Shahoei, M. Li, and J. Yao, "Continuously tunable time delay using an optically pumped linear chirped fiber Bragg grating," *Journal of Lightwave Technology*, vol. 29, no. 10, pp. 1465–1472, 2011.

[22] H. El-Gammal, H. Fayed, A. A. E. Aziz, and M. H. Aly, "Performance analysis & comparative study of uniform, apodized and pi-phase shifted FBGs for array of high performance temperature sensors," *Optoelectronics and Advanced Materials-Rapid Communications*, vol. 9, no. 9-10, pp. 1251–1259, 2015.

[23] S. O. Kasap, "Dispersion in Single- mode fibres," *Optoelectronics and Photonics, Principles and Practices*, pp. 135–146, Pearson Education Limited, London, UK, 2012.

[24] A. B. D. Jha and R. Kumar, "Design and comparative performance analysis of different chirping profiles of tanh apodized fiber Bragg grating and comparison with the dispersion compensation fiber for long-haul transmission system," *Journal of Modern Optics*, vol. 64, no. 6, pp. 1–13, 2016.

[25] N. A. Mohammed and N. M. Okasha, "Single- and dual-band dispersion compensation unit using apodized chirped fiber Bragg grating," *Journal of Computational Electronics*, vol. 17, no. 1, pp. 349–360, 2018.

[26] I. Ashry, A. Elrashidi, A. Mahros, M. Alhaddad, and K. Elleithy, "Investigating the Performance of Apodized Fibre Bragg Gratings for Sensing Applications," in *Proceedings of the 2014 Zone 1 Conference of the American Society for Engineering Education*, Bridgeport, Connecticut, USA, 2014.

[27] A. F. Sayed, F. M. Mustafa, A. A. M. Khalaf, and M. H. Aly, "An enhanced WDM optical communication system using a cascaded fiber Bragg grating," *Optical and Quantum Electronics*, vol. 52, no. 3, pp. 1–21, 2020.

[28] "Optisystem overview," 2022, https://optiwave.com.

[29] S. R. Tahhan, M. H. Ali, M. A. Z. Al-Ogaidi, and A. K. Abass, "Impact of apodization profile on performance of fiber Bragg grating strain–temperature sensor," *Journal of Communications*, vol. 14, no. 1, pp. 53–57, 2019.

[30] I. Nsengiyumva, E. Mwangi, and G. Kamucha, "A comparative study of chromatic dispersion compensation in 10 Gbps SMF and 40 Gbps OTDM systems using a cascaded Gaussian linear apodized chirped fibre Bragg grating design," *Heliyon*, vol. 8, no. 4, Article ID e09308, 2022.